Multiphoton detachment rates of H^- for weak and strong fields

Costas Haritos,[1,*] Theodoros Mercouris,[1,*] and Cleanthes A. Nicolaides[2,1,†]
[1]*Theoretical and Physical Chemistry Institute, Hellenic Research Foundation, Athens 11635, Greece*
[2]*Physics Department, National Technical University, Athens, Greece*
(Received 21 April 2000; published 12 December 2000)

The time-independent Schrödinger problem for the H^- plus ac field system has been solved from first principles via the nonperturbative many-electron, many-photon theory (MEMPT) for a wide range of values of frequency ω and of intensity I of linearly polarized light. The calculations obtained the multiphoton electron detachment rates (MPEDRs) as the imaginary part of a complex eigenvalue and were done for combinations of values of ω and of I defining regimes of ''weak'' and of ''strong'' fields. Most of the results cover the cases of two-, three-,..., seven-photon electron detachment, studied as a function of frequency and of intensity. However, special cases, such as the one of $I=2\times10^{11}$ W/cm^2 for the CO_2 frequency of 0.117 eV, represent detachment processes into various symmetries requiring the absorption of at least 25 photons. The MEMPT results were obtained without any empirical adjustment of energies or of basis sets. The dressed-atom resonance wave function consisted of optimized function spaces for the initial and final states, including the lowest ^1S, $^1P^o$, and ^1D doubly excited states (DES). The initial state was represented by a ten-term numerical multiconfigurational Hartree-Fock wave function whose energy, -0.5275 a.u., is very close to the exact one, -0.5277 a.u., and which accounts self-consistently for electron correlation as well as for the proper magnitude of the $1s$ orbital at large values of r. The H^- DES wave functions were correlated, yielding accurate energies. However, their presence does not affect the results at all. The results converged well when 15 photon blocks were used. In spite of the large number of absorbed photons required in cases such as the CO_2 frequency, the calculations converged well, within the numerical accuracy of the algorithms, by using free-electron angular momenta with 1 up to 7. The systematic quantitative study of the dependence of the MPEDRs on ω and I has led to conclusions as to the behavior at thresholds and as to the limits of validity of the predictions of the lowest-order perturbation theory. An interesting result is the appearance of intensity-dependent structures in the two-, four-, and six-photon detachment rates, which is caused by the interference of the ^1S and ^1D channels. For a number of (I,ω) pairs, comparison is possible with published results obtained by earlier large-scale calculations which either started from first principles or used parametrized one-electron models. Overall, there is good agreement. We conclude that the current level of theoretical knowledge of the H^-MPEDR spectrum is very satisfactory for a large set of experimentally possible laser parameters.

DOI: 10.1103/PhysRevA.63.013410 PACS number(s): 32.80.Rm, 32.80.Gc

I. INTRODUCTION

In order to compute reliably properties related to the nonlinear response of a polyelectronic atomic state, ground or excited, to a laser field, it is necessary to solve the corresponding many-electron, many-photon (MEMP) problem. If the result of the atom-field interaction is an average over many field cycles, there are observables, such as multiphoton electron detachment rates (MPEDRs), which are computable within a time-independent framework. When the expressions of lowest-order perturbation theory (LOPT) produce accurate results for the MPEDRs, the field can be characterized as *weak*. When the LOPT breaks down, the field is said to be *strong*. In this case, either all the necessary higher-order perturbation theory terms have to be computed or the whole approach must be nonperturbative. In all cases, the many-electron part of the problem remains.

Publications from this institute have proposed large-order perturbative as well as nonperturbative approaches for the systematic tackling of the many-electron problem in the presence of an external static or dynamic field. These approaches are based on rigorous formalism and are implemented via computational methods that are characterized by two basic features: The first aims at the use of state-specific wave-function expansions, a fact which allows, via the diagonalization of appropriately constructed matrices, the incorporation of the necessary electronic structure characteristics of ground or excited states. The second involves the extension into the complex energy plane, where the imaginary part of the calculated state-specific energy is the decay rate. The large-order perturbative approach was demonstrated on the calculation of LoSurdo-Stark shifts and widths not only of the ground state but also of excited states of hydrogen [1], where one of the difficulties that had to be resolved is how to handle rigorously and efficiently the zero-order degeneracy. The nonperturbative approach has been implemented for the calculation of energy shifts and widths in magnetic fields, with applications to hydrogen and to doubly excited states (DES) of H^- [2]. Its most extensive implementation has been for the calculation of properties induced by dc and ac electric fields, with applications to a number of small atoms in ground or excited states ([3,4] and references therein).

It is the nonperturbative MEMP theory (MEMPT) ([3]

*Electronic address: thmerc@eie.gr
†Electronic address: can@eie.gr

and references therein) that we apply here to the two-electron H^- for the calculation of MPEDRs for a wide range of field frequencies ω and intensities I of linearly polarized light. Specifically, these cover the ranges from $\omega=0.114$ to 0.843 eV and from $I=1.0\times10^9$ to 1.1×10^{12} W/cm^2. Combinations of values from these two sets of parameters define situations of weak as well as of strong-field interactions and of electron detachment requiring the absorption of many photons, reaching a case of 25 photons when I becomes 2×10^{11} W/cm^2 for the CO_2 frequency of 0.117 eV. (1 a.u., of energy for H^- $=27.1966$ eV).

Most of the herein MEMPT results constitute predictions, complementing the information on the multiphoton electron detachment processes in H^- already in the literature. Some of this information is experimental (e.g., [5]). However, most of it is theoretical and, where possible, we compare with earlier theoretical MPEDRs [6].

During the past two decades, the system ''H^- plus laser field'' has been treated in terms of two categories of approaches as regards the way electronic structure and the spectrum are accounted for. In the first category are calculations which were done from first principles by perturbative or nonperturbative methods. In the second category are calculations which were done by employing one-electron parametrized models. The replacement of the two-electron problem (or, of the many-electron problem for larger negative ions) by a one-electron model, where the binding energy is taken from other calculations or from experiment and where the wave functions are adjusted according to the model, facilitates the calculation of MEPDRs and offers the opportunity for extensive computations with good overall accuracy. Nevertheless, the fact remains that such models cannot form a basis for a general methodology toward the understanding of the interplay between the parameters of the laser field and the characteristics of atomic spectra and atomic structure. For example, even for the simple case of the H^- spectrum, when the two-electron ^1S ground state is replaced by models of an s electron, the roles of angular correlation or of DES remain unknown.

The justification and the methods of the MEMPT are presented in detail in Ref. [3] and references therein, and only a brief review will be given here (Sec. II). The essential result of a MEMPT calculation is a complex eigenvalue and the corresponding eigenfunction, representing the field-dressed resonance state. The computation is based on a superposition of state-specific eigenfunctions with judiciously chosen function spaces of real and complex orbitals, allowing formally and practically the systematic calculation of the effects of electronic structure, of electron correlation, of multiply excited states, and of interchannel coupling, occurring in the discrete and in the continuous spectrum. No empirically adjusted parameters for potentials, for shifted or unshifted energies, or for basis sets are necessary.

The development and first applications of the MEMPT were carried out in the 1980s on two prototypical negative ions, H^- and Li^- [6–12]. Specifically, for the calculation of MPEDRs of H^-, we considered the case of linearly polarized light of frequencies in the range 0.004 00–0.004 30 a.u. (CO_2 laser) and of intensities $0.7\times10^9-1.25\times10^{10}$ W/cm^2 [6,7], a situation which is achievable in the laboratory. Given that the detachment threshold of H^- is 0.027 75 a.u. (0.755 eV), the use of the CO_2 laser frequencies around 0.004 30 a.u. ($\omega=0.117$ eV, $\lambda\approx105\,900$ Å) implies a seven-photon detachment process in the weak-field regime where the energy shifts are insignificant. The initial application of the MEMPT also produced results for frequencies requiring a minimum of one, two, or three photons for electron detachment with unshifted energies [9]. Using a correlated wave function for the initial state, attention was paid to the calculation of observable phenomena caused by the field-dressed interchannel coupling in the final state, without and with the presence of a dc field, for laser intensities in the range $0.5\times10^{10}-0.7\times10^{11}$ W/cm^2. For example, in the frequency region of the two-photon detachment threshold, an intensity-dependent effect was found which was attributed to ''*field-induced coupling and interference between the continuum* ^1S *and* ^1D *channels*'' (Fig. 4 of [9]). Also found was that the simultaneous mixing of a parallel dc field increases the nonperturbative character of the spectrum of the above threshold detachment [11]. The solution of the quantum-mechanical problem for H^- in the presence of parallel dc and ac fields also produced quantitatively the oscillations in the detachment rate as a function of frequency, a phenomenon which had earlier been observed experimentally [5(b)] and predicted only via semiclassical calculations ([8,9] and references therein). Finally, it was concluded that the proper representation of the perturbed final state, i.e., of the dressed free electron in a short-range potential, is crucial for obtaining accurate results. For basis expansion-type methods this implies making certain that convergence as a function of angular momenta in the continuous spectrum has been achieved. These findings provided a reasonable explanation [8,9] for the then existing qualitative discrepancy in two-photon detachment rates between the previous *ab initio* calculations [13,14] and calculations based on model potentials with perturbed free-electron orbitals [15,16].

The early MEMPT results on MPEDRs of H^- have been compared in the literature with results obtained by other methods, perturbative or nonperturbative. For example, such comparisons were presented by Mercouris and Nicolaides [9,6] for two- and three-photon rates and generalized cross sections, the latter having been deduced from the nonperturbative MEMPT calculations for values of the intensity assumed to be in or near the weak-field regime. It was shown [9(b)] that there is reasonable agreement between the MEMPT results and the model ones by Geltman [17]. Overall agreement with the early MEMPT results was also reported by Liu, Gao, and Starace [18], who employed a variationally stable procedure at the LOPT level with empirical energy differences and adiabatic hyperspherical functions. On the other hand, serious discrepancies were observed when Dörr *et al.* [19] published their results and compared with the MEMPT ones for CO_2 laser frequencies [6,7]. The authors of [19] implemented Floquet theory at the level of a one-electron model, and Keldysh-type theories at the level of one and two electrons, for rates at the CO_2 laser frequency of 0.117 eV. We now know that the MEMPT results of [7,6] for intensities smaller than about 1×10^{10} W/cm^2 are not accu-

rate. That application contained intrinsic numerical errors due to the smallness of the rates, i.e., of the imaginary part of the complex eigenvalues, and led to false indications of convergence when the field strength was on the low side. (In [7], the region of intensities between 10^9 and 10^{10} W/cm^2 was chosen so as to be in the vicinity of the perturbative regime on the low side and to the closing of the seven-photon channel on the high side. Furthermore, this range was suitable for the experimental capabilities of the time). Since the available computer power was then very restricted, numerical experimentation and extensive optimization of the function spaces while searching for stability of the complex eigenvalue, was not done. MEMPT results for the CO_2 laser frequencies 0.114, 0.117, and 0.120 eV for intensities $1\times10^{10}-2\times10^{11}$ W/cm^2 are presented here.

The structure of the paper is as follows: In Sec. II we outline the essential features of the MEMPT. In Sec. III we discuss the function spaces used in the calculations. In Sec. IV we present the MEMPT results, some of which are compared with available previous theoretical results. The dependence of the MPEDRs on frequency as well as on intensity is revealed in a quantitative way. Section V is our conclusion.

II. BRIEF REVIEW OF THE MEMPT

The MEMPT aims at making the *ab initio* nonperturbative calculation of field-perturbed states and of quantities representing the cycle-averaged nonlinear response of atoms and molecules to strong static and dynamic electromagnetic fields, feasible and physically transparent for arbitrary N-electron states. To this effect we choose trial wave functions where the function spaces are optimized appropriately and are as state-specific as possible. This allows a practical understanding of the contribution of different parts of the wave function and of the spectrum, a fact which, apart from improved convergence, facilitates the transfer of meaningful information from a MEMPT calculation on the spectrum of one system to that of another.

The key features and computational steps are as follows.

(1) The framework is time independent and employs the ''*atom plus field*'' Hamiltonian in the dipole approximation, which, for linearly polarized monochromatic light along the z axis is, in a.u.,

$$H_{\rm ac}=H_{\rm atom}+\omega\alpha_\omega^\dagger a_\omega-\tfrac{1}{2}F_{\rm ac}z(\alpha_\omega^\dagger+\alpha_\omega). \tag{1}$$

ω is the field frequency, $\alpha_\omega^\dagger(\alpha_\omega)$ are the photon creation (annihilation) operators, and $F_{\rm ac}$ is the electric-field strength $(1\ \text{a.u.}=5.14\times10^9\ \text{V/cm})$.

(2) The problem of computing the MPEDR to all orders is formulated as follows: Using the $H_{\rm ac}$ of Eq. (1) and a properly chosen set of N-electron function spaces consisting of real as well as of complex one-electron basis sets, a state-specific complex eigenvalue matrix equation is constructed, whose form and method of solution are given in [3,9,10] and are not repeated here. The sought-after complex eigenvalue corresponds to the resonance state resulting from the field-induced mixing of all physically significant field-free states of the discrete and the continuous spectrum. The detachment rate corresponds to the imaginary part of this eigenvalue for each value of ω and I.

(3) In order to secure accuracy and reliable convergence, it is necessary to start with an accurate wave function for the unperturbed initial state. In the case of problems such as the present one, the calculation for the bound wave functions, including that for the initial state, is carried out according to the state-specific theory ([20] and references therein). Once the correlated wave functions for the most significant localized states are computed, we estimate what types of, and how many, real and virtual states will contribute via (1) to all orders. This estimate is, of course, only an approximation. The final solution is obtained by the systematic addition or subtraction of terms and of parameter optimization until convergence is established.

(4) The overall calculation for a particular state, or a set of states of interest, searches for the following.

(i) A frequency- and intensity-dependent square-integrable N-electron wave function, $\Psi(r;\rho^*)$, which is connected directly to the unperturbed wave function $\Psi_0(r)$ and has maximum overlap with it. The letter r stands for the real coordinates of electrons in states which are bound. The complex coordinate $\rho^*=re^{-i\theta}$ is the coordinate in the Gamow orbital of the outgoing electron. The form of the MEMPT wave function for single-electron ejection is

$$\Psi(r;\rho^*)=\sum_{i,,n}\alpha_{i,n}(\theta)|\Psi_i(r_N);n\rangle + \sum_{i,,n}\alpha_{j,n}(\theta)|X_j(r_{N-1},\rho^*);n\rangle. \tag{2}$$

Ψ_i denotes discrete bound states (including the initial one Ψ_0) and the localized parts of autoionizing states. X_j denotes unbound states in the continuous spectrum represented by complex L^2 wave functions. $|n\rangle$ denotes the photon states. r_{N-1} and r_N represent collectively the real coordinates of the wave functions for the $(N-1)$- electron core for each channel j and for the N-electron bound and autoionizing states. The magnitude of the contribution of each of the wave functions in the expansion (2) to the determination of the energy shift and width depends, weakly or strongly, on ω and $F_{\rm ac}$.

(ii) A state-specific complex eigenvalue

$$z_0(\omega,F_{\rm ac})=E_0+\Delta(\omega,F_{\rm ac})-\frac{i}{2}\Gamma(\omega,F_{\rm ac}), \tag{3}$$

where the energy shift Δ and decay width Γ are small compared to the unperturbed energy E_0, and z_0 is connected to E_0 smoothly as a function of the laser parameters ω and $F_{\rm ac}$.

(5) Given the structure of the MEMPT wave function, Eq. (2), the computational search for z_0 has two major phases. The first involves the calculation of accurate state-specific representations of the field-free discrete and autoionizing N-electron states and of the term-dependent channel states of the $(N-1)$-electron core. In general, the wave functions are made up of a zero-order part, computed at the Hartree-Fock (HF) or multiconfigurational HF (MCHF) level, and of a

correlation correction part. The advantages of solving the many-electron problem for each ground or excited state in this way are discussed in [20].

The second phase involves the calculation of the mixing coefficients in Eq. (2) via the repeated diagonalization of H_{ac} and the optimization of the rotated Gamow orbitals which are coupled to the core wave functions for each channel j and for each ''Floquet'' block in the H_{ac} matrix, representing real and virtual photons, absorbed or emitted. The number of complex radial functions [Eqs. (9)–(11)] and of angular momenta are augmented systematically, until stability of the complex eigenvalue z_0 is observed as a function of a nonlinear parameter in the basis set and of the rotation angle θ.

Presently, it is not possible to decide *a priori* on the range of values of the field strength (for each frequency) for which accurate results can be obtained for a given N-electron state. However, we do know that there are serious difficulties for weak and for very strong fields. In the first case, the problem is purely numerical, since the imaginary part of z_0 becomes extremely small. For widths smaller than 10^{-11} a.u., we have found that these MEMPT calculations either may lead to unreliable solutions or cannot produce stable solutions at all. Of course, rates in such regions are computable by LOPT, provided the many-electron problem is handled correctly, and there is no need for the application of nonperturbative theory. In the second case, the spectrum is distorted, and the correct correspondence between E_0 and z_0 and between Ψ_0 and Ψ may either become fuzzy or even disappear, while more than one complex roots may appear in the same neighborhood. In the present work, all solutions that are reported were identified clearly, whether the field was weak or strong.

III. CHOICE OF FUNCTION SPACES FOR THE PRESENT CALCULATIONS

The Ψ_i of Eq. (2) consisted of wave functions for the ^1S ground state and for the lowest-lying doubly excited resonances of ^1S, $^1P^o$, and ^1D symmetry. In fact, the calculations were carried out without and with electron correlation in the ground state and without and with the presence of the two-electron resonances in order to determine their contribution. The results of this study are reported elsewhere [21]. Here we present the final results which are obtained from the use of well-correlated wave functions for these states.

The ^1S ground state was represented by a ten-term MCHF wave function whose orbitals were obtained numerically from Froese-Fisher's code [22]. For a small system such as H^-, this calculation is economic and the resulting wave function not only is compact but also accurate. Hence, there is no need to include additional correlation variationally in terms of analytic virtual orbitals as is usually done in the framework of the state-specific theory [20]. The MCHF H^- ^1S wave function which was used is

$$\begin{aligned}\Psi_0 = {} & \alpha_1\psi(1s^2)+\alpha_2\psi(2s^2)+\alpha_3\psi(3s^2)+\alpha_4\psi(4s^2)\\ & +\alpha_5\psi(2p^2)+\alpha_6\psi(3p^2)+\alpha_7\psi(4p^2)+\alpha_8\psi(3d^2)\\ & +\alpha_9\psi(4d^2)+\alpha_{10}\psi(4f^2),\end{aligned} \tag{4}$$

whose energy is $E=-0.5275$ a.u. (The accurate value for the energy of H^- is $E=-0.5277$ a.u.) The values of the coefficients are

$$\begin{gathered}\alpha_1=0.971,\quad \alpha_2=-0.208,\quad \alpha_3=-0.014,\\ \alpha_4=-0.003,\quad \alpha_5=-0.110,\\ \alpha_6=-0.016,\quad \alpha_7=-0.004,\quad \alpha_8=-0.018,\\ \alpha_9=-0.005,\quad \alpha_{10}=0.006.\end{gathered} \tag{5}$$

From Eqs. (4) and (5) it is evident that the major structure features which contribute to the H^- properties are represented by the $1s^2$ configuration, by the $2s^2$ radial correlation, and by the $2p^2$ angular correlation, with orbitals optimized self-consistently. Such a wave function was used in the first MEMPT calculations as well [9(a)]. A systematic analysis of the connection between the wave-function characteristics of the initial state of H^- and of the MEPDRs showed that the dominant effect of angular and of radial correlation on the MPEDRs is via the changes they cause, self-consistently, on the magnitude of the $1s$ orbital for large values of its coordinate [21].

We now come to the calculation of wave functions for the lowest-lying DES of ^1S, $^1P^o$, and ^1D symmetry. According to the state-specific theory for autoionizing states ([20], and references therein), the optimal representation of the main part of the localized component is achieved compactly via a MCHF calculation subject to appropriate orthogonality constrains. Although this is not the place to discuss the state-specific theory and methods of computation of multiply excited states (see [20,23] and references therein), it is useful to point out the following: A successful calculation of a bound MCHF wave function, whose energy is in the continuous spectrum and which is expected to be a good zero-order representation of the exact wave function, depends crucially on the accuracy of the numerical techniques and on the choice of the configurations in terms of which the MCHF equations are constructed. In doing so, two criteria are important. The first is the magnitude of the mixing coefficient. Here we note that orbital transformations are often useful and even necessary in order to obtain a correct convergence. The second is the way that certain configurations facilitate the solution of the MCHF equations, regardless of the size of their mixing coefficient. A well-known example from the MCHF theory of low-lying discrete states is the calculation of the He $1s2s$ ^1S wave function and energy. In order to achieve proper convergence, the MCHF calculation must contain the $1s^2$ configuration as well, even though its mixing coefficient is small, about 0.11. Otherwise, in the absence of the $1s^2$ configuration, the energy of the final solution is below the exact one, even at the single-configuration HF level ($1s2s$).

For the case of H^-, it turns out that the numerical MCHF equations lead to properly converged state-specific solutions only for the ^1S and ^1D states, for which the following wave functions and energies were obtained:

TABLE I. Nonperturbative multiphoton electron detachment rates (MPEDRs) (in a.u.) of H^- at the CO_2 laser frequency (0.117 eV) for intensities in the range 1.0×10^{10}–1.0×10^{11} W/cm^2. The MPEDR for this work is equal to Γ of the complex eigenvalue of Eq. (3). For Ref. [19]: (a) Floquet calculations with a parametrized one-electron potential; (b) Keldysh formula with a Hylleraas ground-state wave function; (c) Faisal-Reiss formulas with a Hylleraas wave function. For Ref. [24]. Floquet calculations with a parametrized one-electron potential.

	Photodetachment Rate (a.u.)		
Intensity (W/cm^2)	MEMPT (This work)	Ref. [19]	Ref. [24]
1.0×10^{10}	$1.038(\pm0.12)\times10^{-9}$		0.966×10^{-9}
1.12×10^{10}	$2.044(\pm0.11)\times10^{-9}$	2.7×10^{-9} (a)	
		8.8×10^{-10} (b)	
		2.1×10^{-9} (c)	
2.52×10^{10}	$1.12(\pm0.08)\times10^{-7}$	1.4×10^{-7} (a)	
		5.1×10^{-8} (b)	
		1.0×10^{-7} (c)	
5.0×10^{10}	$1.81(\pm0.06)\times10^{-6}$		1.67×10^{-6}
10.0×10^{10}	$1.68(\pm0.03)\times10^{-5}$		1.61×10^{-5}

$$\Phi_0(^1S)=0.815\psi(2s^2)-0.075\psi(3s^2)-0.567\psi(2p^2)-0.074\psi(3p^2)-0.047\psi(3d^2), \quad (6)$$

$E_0(^1S)=9.554$ eV above H $1s$, and

$$\Psi_0(^1D)=0.851\psi(2p^2)-0.450\psi(2s3d)-0.250\psi(3p^2)-0.083\psi(3d^2), \quad (7)$$

$E_0(^1D)=10.147$ eV above H $1s$.

These energies compare very well with the ones obtained from complete calculations, including the small shift from the contribution of the open channels. [$E(^1S)=9.552$ eV, $E(^1D)=10.199$ eV] [23]. (Reference [23] discusses the resolution of the H^- resonance spectrum up to the $n=4$ or 5 thresholds and compares with available results for low-lying DES).

The $^1P^o$ spectrum contains Feshbach resonances just below the $n=2$ threshold and one shape resonance just above it, at 10.215 eV above the H $1s$ threshold. The lowest $^1P^o$ resonance below the $n=2$ threshold is at 10.173 eV [23]. Since the MCHF equations did not produce a reliably converged solution for these $^1P^o$ states, we resorted to a more approximate representation by diagonalizing the energy matrix constructed from full configuration interaction with hydrogen orbitals $2s,2p,3s,3p,3d,4s,4p,4d$, and using the wave functions of the two lowest roots, which are at 10.201 and 10.240 eV above the H $1s$ threshold.

The X_j of Eq. (2) were obtained as a product of the $1s$ core orbital and a Gamow orbital,

$$X_j(\rho)=\psi(1s)\otimes\varepsilon l(\theta). \quad (8)$$

$\varepsilon l(\theta)$ has orbital angular momentum l and is expanded in terms of a square integrable basis set of STO's,

$$\varepsilon l(\theta)=\sum_n c_n^{(l)}(\theta)f_n^{(l)}(\rho^*), \quad (9)$$

where

$$f_n^{(l)}(r)=r^{l+n-1}e^{-ar} \quad \text{with} \quad n=1,2,3,...,12 \quad \text{and}$$

$$l=0,1,...,7. \quad (10)$$

Given the range of values of ω and I, and the fact that the $n=2$ excited states are 10.2 eV above the $1s$ state, no field-induced excitations of the core $1s$ orbital were considered. The exponent a in Eq. (10) was optimized and the final value, for which a range of stable results was obtained, is $a=0.20$.

We found that good convergence is obtained in general when 15 photon blocks are included. In spite of the large number of absorbed photons required in cases such as the CO_2 frequency, the calculations converged well, within the numerical accuracy of the algorithms, by using electron angular momenta 1 up to 7. Test calculations showed that expansions with 1 up to 9 made only a slight difference from those obtained with momenta 1 up to 7 of the order of 0.5–2 %.

Convergence and stability of the complex eigenvalue value is easier when ω is large. When the rates get small, of the order of 10^{-9}–10^{-10} a.u., changes in the number of photon blocks cause a greater change, percentage-wise. For example, for $\omega=0.117$ eV, when the rate is 1×10^{-9} a.u. the estimated error is 11%, whereas when intensity increases and brings the rate to 1.8×10^{-6} a.u., the error is only 3% (see Tables I and II). The results were stable when the variation of the rotation angle θ is between 17°–25°. In general, in the region near a threshold, convergence and stability of results are more difficult than otherwise.

TABLE II. MPEDRs of H^- for the MEMPT for CO_2 frequencies and intensities up to 2.0×10^{11} W/cm^2. The error margins are deduced from the behavior of convergence as a function of the number of photons blocks.

	Photodetachment Rates (a.u.)		
Intensity (W/cm^2)	0.114 eV	0.117 eV	0.120 eV
5×10^{10}	$1.780(\pm0.060)\times10^{-6}$	$1.810(\pm0.060)\times10^{-6}$	$1.851(\pm0.070)\times10^{-6}$
7×10^{10}	$0.560(\pm0.024)\times10^{-5}$	$0.565(\pm0.024)\times10^{-5}$	$0.569(\pm0.024)\times10^{-5}$
1.2×10^{11}	$0.279(\pm0.002)\times10^{-4}$	$0.282(\pm0.002)\times10^{-4}$	$0.283(\pm0.002)\times10^{-4}$
1.4×10^{11}	$0.408(\pm0.002)\times10^{-4}$	$0.410(\pm0.002)\times10^{-4}$	$0.411(\pm0.002)\times10^{-4}$
1.6×10^{11}	$0.588(\pm0.002)\times10^{-4}$	$0.591(\pm0.002)\times10^{-4}$	$0.592(\pm0.002)\times10^{-4}$
1.8×10^{11}	$0.780(\pm0.002)\times10^{-4}$	$0.782(\pm0.002)\times10^{-4}$	$0.785(\pm0.002)\times10^{-4}$
2.0×10^{11}	$0.994(\pm0.001)\times10^{-4}$	$0.997(\pm0.001)\times10^{-4}$	$1.001(\pm0.001)\times10^{-4}$

IV. MEMPT RESULTS AND COMPARISON WITH AVAILABLE DATA

A. CO_2 frequencies around $\omega=0.0043$ a.u.

We start with the results for the MPEDRs using three frequencies of the CO_2 laser, 0.0042, 0.0043, and 0.0044 a.u., and eleven values of intensity in the range 1×10^{10} W/cm^2–2×10^{11} W/cm^2. These MEMPT results replace the ones that were published in [7] and which, for numerical reasons, are inaccurate, except the ones for $I=1.25\times10^{10}$ W/cm^2 [6]. Through the present study we established that only when the rates are larger than about 10^{-11} a.u. (1 a.u.$=4.13\times10^{16}$ sec^{-1}) is the stability of the complex eigenvalue, as obtained by the MEMPT algorithms, reliable. Our results, computed using the wave functions discussed in Sec. III, are contained in Tables I and II. They are assigned error margins which are deduced by following convergence as a function of the number of the photon blocks. Specifically, these error margins stand for the maximum deviation of the rates from their average value in the range of 14 to 16 photon blocks, which is the region where convergenge is reached. It can be seen that this margin narrows with increasing intensity and consequent increase of the rate.

Table I also compares the MEMPT results with those of [19,24] for frequency $\omega=0.0043$ a.u. (0.117 eV) and intensity values, used in [19,24], in the range 1×10^{10} W/cm^2–10×10^{10} W/cm^2. This range corresponds to the strong-field regime, since perturbation theory breaks down already below 1×10^{10} W/cm^2 [19]. Electron detachment takes place with the absorption of more than seven photons, where the extra photons are needed because of the ponderomotive energy shifts. In the column for Ref. [19], we have included the results of three types of calculations (Table II of [19]). The first is from ''Floquet'' theory with a Yukawa-type one-electron model potential, whose results the authors considered as the benchmark for all the calculations that they did. The second type is from two-electron Keldysh theory with a 24-parameter Hylleraas wave function for the initial state, and the third type is from the Faisal-Reiss variation of Keldysh theory, again with the same correlated wave function for H^-. The numbers in the column for Ref. [24] in Table I are results of computations using Floquet theory and a pseudospectral method for discretizing the dressed Hamiltonian, in conjunction with a parametrized one-electron model potential.

The agreement of the MEMPT results with those of Telnov and Chu [24] for the intensities 1×10^{10}, 5×10^{10}, and 10×10^{10} W/cm^2 is very good. This is satisfying, considering that the calculations of [24] used large basis sets and substantial empirical input. As regards the comparison with the results of the three methods applied by Dörr *et al.* [19], the MEMPT results are in very good agreement with those obtained from the Faisal-Reiss formulas, and in general agreement (within a factor of 2 for the worst case), with those from the other two types.

Table II contains the MEMPT results for three frequencies, 0.114, 0.117, and 0.120 eV, and for seven intensity values, up to 2.0×10^{11} W/cm^2. These predictions may be of use to future experimental investigations.

B. Electron detachment by one, two, and three photons

Most of the existing calculations for the MPEDRs of the H^- ^1S state are for frequencies and intensities that are capable of ejecting one electron by one, two, or three photons. Our results for this region are presented in Figs. 1(a)–1(e), and in Tables III and IV for various values of ω and I.

In Table III we compare with the previous MEMPT results of Mercouris and Nicolaides (Table III of [9(a)]) for a range of frequencies from 0.0098 to 0.0500 a.u. and for $I=0.7\times10^{11}$ W/cm^2. Note that we report the half-widths for the correct value of the intensity [6]. This comparison supports the validity of the early MEMPT results in a satisfactory way, considering the fact that our computer capacity was much more limited at that time. The main characteristics of the behavior of the MPEDRs for this frequency range were predicted in [9(a)] and are verified by the present MEMPT results. These characteristics are the following: Before the three-photon channel opens at $\omega=0.0106$ a.u., there is a minimum of the rate at $\omega=0.0105$ a.u. and then a jump, right after the opening of the channel. In the frequency region between the three-photon threshold and the two-photon threshold at $\omega=0.0149$ a.u., the rate falls by a factor of 5. With the opening of the two-photon channel, the rate rises again sharply at $\omega=0.016$ a.u. followed by a new decrease, until $\omega=0.028$ a.u., where the one-photon channel opens. This picture of the dependence of MPEDRs on frequency,

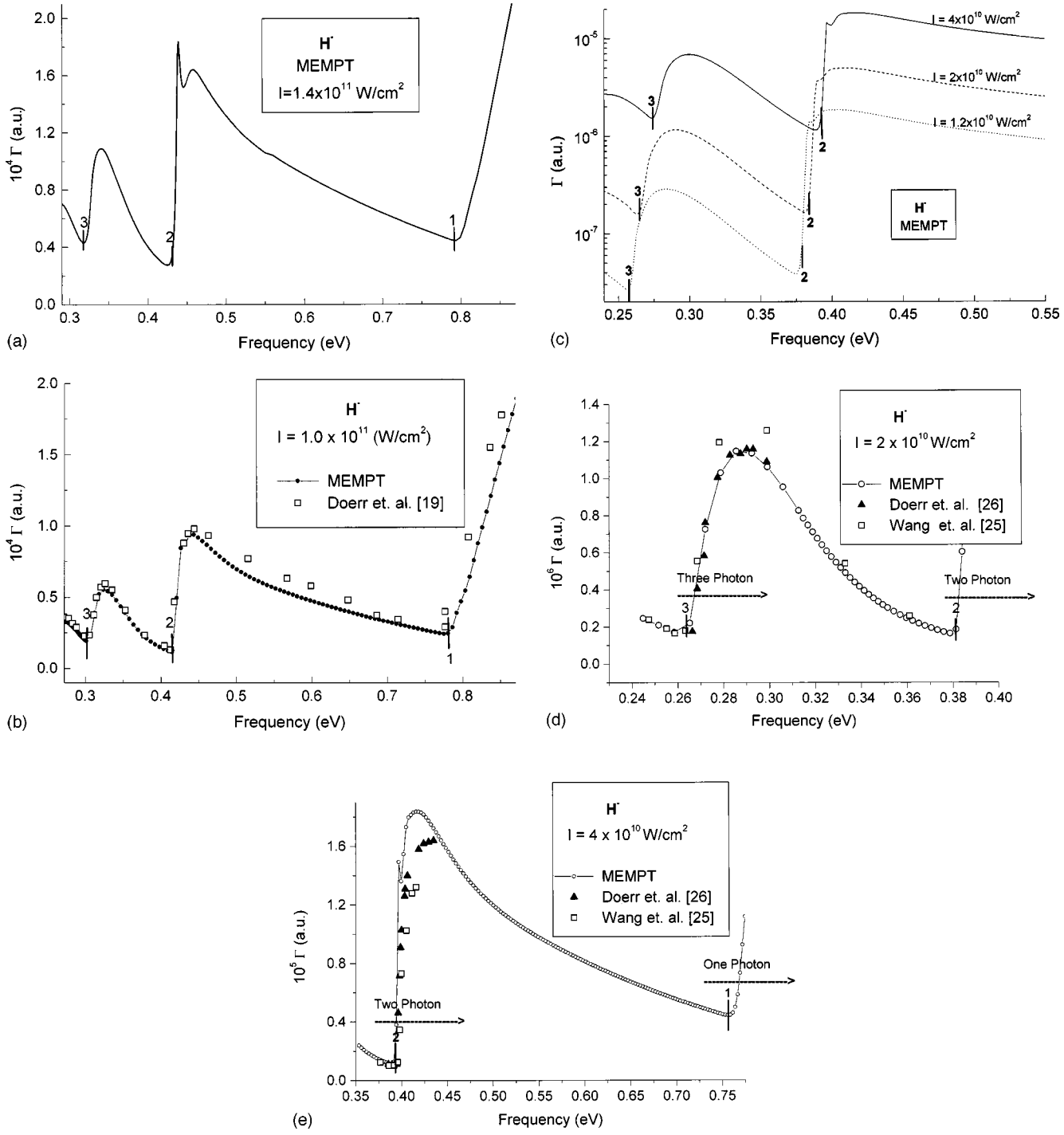

FIG. 1. (a) MPEDRs Γ [see Eq. (3), in a.u.] for $I=1.4\times10^{11}\,\mathrm{W/cm^2}$ in the frequency region covering mainly three- and two-photon detachment. The threshold energies are indicated by the numbered lines on the graph. The structure above the two-photon threshold is due to the interference between the ^1S and ^1D channels. (b) MPEDRs (in a.u.) for $I=1.0\times10^{11}\,\mathrm{W/cm^2}$ in the frequency region covering mainly three- and two-photon detachment. The Floquet one-electron model results of Dörr *et al.* [19] are also shown. At this intensity, the two-photon threshold structure shown in (a) is very weak. (c) MPEDRs (in a.u.) from the present MEMPT calculations for three values of intensity in the frequency range where three- and two-photon electron detachment occurs. Note that the three-photon rate rises at threshold sharply and falls rapidly with frequency. (d) Comparison of the MEMPT results for three-photon electron detachment rates at $I=2.0\times10^{10}\,\mathrm{W/cm^2}$, with two other nonperturbative calculations. (e) Same as (d) for two-photon electron detachment rates and $I=4.0\times10^{10}\,\mathrm{W/cm^2}$. The MEMPT reveals structure at the two-photon threshold due to the ^1S-^1D channel interference.

TABLE III. MPEDRs ($\Gamma/2$ in a.u.) of H^- from two MEMPT calculations (Ref. [9(a)] and this work), covering mainly the energy range for three- and two-photon electron detachment at $I=7.0\times10^{10}$ W/cm^2. The three-photon threshold is at $\omega=0.0107$ a.u. and the two-photon threshold is at $\omega=0.0149$ a.u. See [6].

	$\Gamma/2$ (a.u.)	
Frequency (a.u.)	Ref. [9(a)]	This work
0.0098	0.712×10^{-5}	0.623×10^{-5}
0.0100	0.652×10^{-5}	0.574×10^{-5}
0.0105		0.410×10^{-5}
0.0110	0.115×10^{-4}	0.883×10^{-5}
0.0115		0.128×10^{-4}
0.0120	0.130×10^{-4}	0.114×10^{-4}
0.0121		0.109×10^{-4}
0.0125		0.891×10^{-5}
0.0130	0.743×10^{-5}	0.655×10^{-5}
0.0135		0.480×10^{-5}
0.0140	0.404×10^{-5}	0.354×10^{-5}
0.0144		0.280×10^{-5}
0.0160	0.282×10^{-4}	0.251×10^{-4}
0.0180	0.211×10^{-4}	0.190×10^{-4}
0.0200	0.168×10^{-4}	0.149×10^{-4}
0.0250	0.101×10^{-4}	0.905×10^{-5}
0.0275	0.764×10^{-5}	0.698×10^{-5}
0.0325	0.923×10^{-4}	0.750×10^{-4}
0.0375	0.158×10^{-3}	0.136×10^{-3}
0.0425	0.176×10^{-3}	0.155×10^{-3}
0.0475	0.171×10^{-3}	0.154×10^{-3}
0.0500	0.165×10^{-3}	0.150×10^{-3}

should be normal for a simple spectrum of a negative ion and for intensities which are not strong.

Comparison with results of other types of nonperturbative calculations is done in Figs. 1(b), 1(d), and 1(e) and in Table IV, whilst a comparison with results from LOPT is done in Sec. IV F. In Fig. 1(b), we show the MEMPT results for $I=1\times10^{11}$ W/cm^2 in the region of one-, two-, and three-photon detachment and we compare with [19]. The agreement is very good. We note that Dörr *et al.* [19] found that LOPT begins to break down between the thresholds for one- and two-photon detachment. Figure 1(c) presents the MEMPT rates for $I=(1.2\times10^{10}, 2\times10^{10}$, and 4×10^{10} W/cm^2) in the frequency range of 0.23–0.55 eV (two- and three-photon detachment). Note that the structures at threshold depend on intensity, in agreement with the early results of [9(a)]. These results compare very well with those of [19,25] even though it is not possible to detect in their figures, where the rates are given on logarithmic scale, whether the same threshold detail is present there. Wang, Chu, and Laughlin [25] used Floquet theory with a one-electron model and Floquet matrices reaching dimensions of about $10\,000\times10\,000$ for $I=4\times10^{10}$ W/cm^2. Their results showed intensity-dependent variations near the onset of the detachment thresholds, in agreement with the predictions published in [9(a)]. (See Fig. 4 of [9(a)] for the two-photon detachment rate in the range $I=0.55\times10^{10}$ W/cm$^2-7\times10^{10}$ W/cm^2 [6]). Wang *et al.* [25] also made a detailed analysis of the experimental data by Tang *et al.*, Balling *et al.*, and Bryant *et al.* [5] and concluded that the proper interpretation of the measured processes requires a nonperturbative treatment.

Figures 1(d) and 1(e) present our MEMPT results for $I=2\times10^{10}$ W/cm^2 and $I=4\times10^{10}$ W/cm^2 and compare them to those of Wang *et al.* [25] as well as of Dörr *et al.* [26], the latter obtained from *R*-matrix Floquet calculations. The mag-

TABLE IV. MPEDRs of H^- (in a.u.) from three nonperturbative calculations for three laser frequencies and 15 values of intensity.

	Photodetachment Rate (a.u.)					
Intensity	0.650 eV		0.755 eV		1.164 eV	
(W/cm^2)	This work	Ref. [28]	This work	Ref. [28]	This work	Ref. [27]
1×10^9	4.33×10^{-9}	4.85×10^{-9}		6.33×10^{-9}	4.51×10^{-6}	4.66×10^{-6}
4×10^9	6.95×10^{-8}				1.80×10^{-5}	
8×10^9	2.78×10^{-7}				3.60×10^{-5}	
1×10^{10}	4.33×10^{-7}	4.80×10^{-7}	5.05×10^{-7}	2.98×10^{-7}	4.50×10^{-5}	4.65×10^{-5}
5×10^{10}	1.04×10^{-5}		6.82×10^{-6}		2.20×10^{-4}	
8×10^{10}	2.58×10^{-5}		1.71×10^{-5}		3.56×10^{-4}	
1×10^{11}	3.98×10^{-5}	4.37×10^{-5}	2.63×10^{-5}	2.78×10^{-5}	4.43×10^{-4}	4.53×10^{-4}
2×10^{11}	1.46×10^{-4}	1.58×10^{-4}	0.99×10^{-4}	1.05×10^{-4}	8.70×10^{-4}	
3×10^{11}	3.01×10^{-4}		2.10×10^{-4}		1.28×10^{-3}	
4×10^{11}	4.95×10^{-4}	5.30×10^{-4}	3.55×10^{-4}	3.76×10^{-4}	1.66×10^{-3}	
6×10^{11}	9.78×10^{-4}		7.19×10^{-4}		2.38×10^{-3}	
8×10^{11}	1.55×10^{-3}	1.52×10^{-3}	1.15×10^{-3}	1.23×10^{-3}	2.98×10^{-3}	
9×10^{11}	1.88×10^{-3}		1.40×10^{-3}		3.24×10^{-3}	
1×10^{12}	2.12×10^{-3}	2.18×10^{-3}	1.64×10^{-3}	1.73×10^{-3}	3.46×10^{-3}	2.95×10^{-3}
1.1×10^{12}	2.40×10^{-3}		1.90×10^{-3}		3.65×10^{-3}	

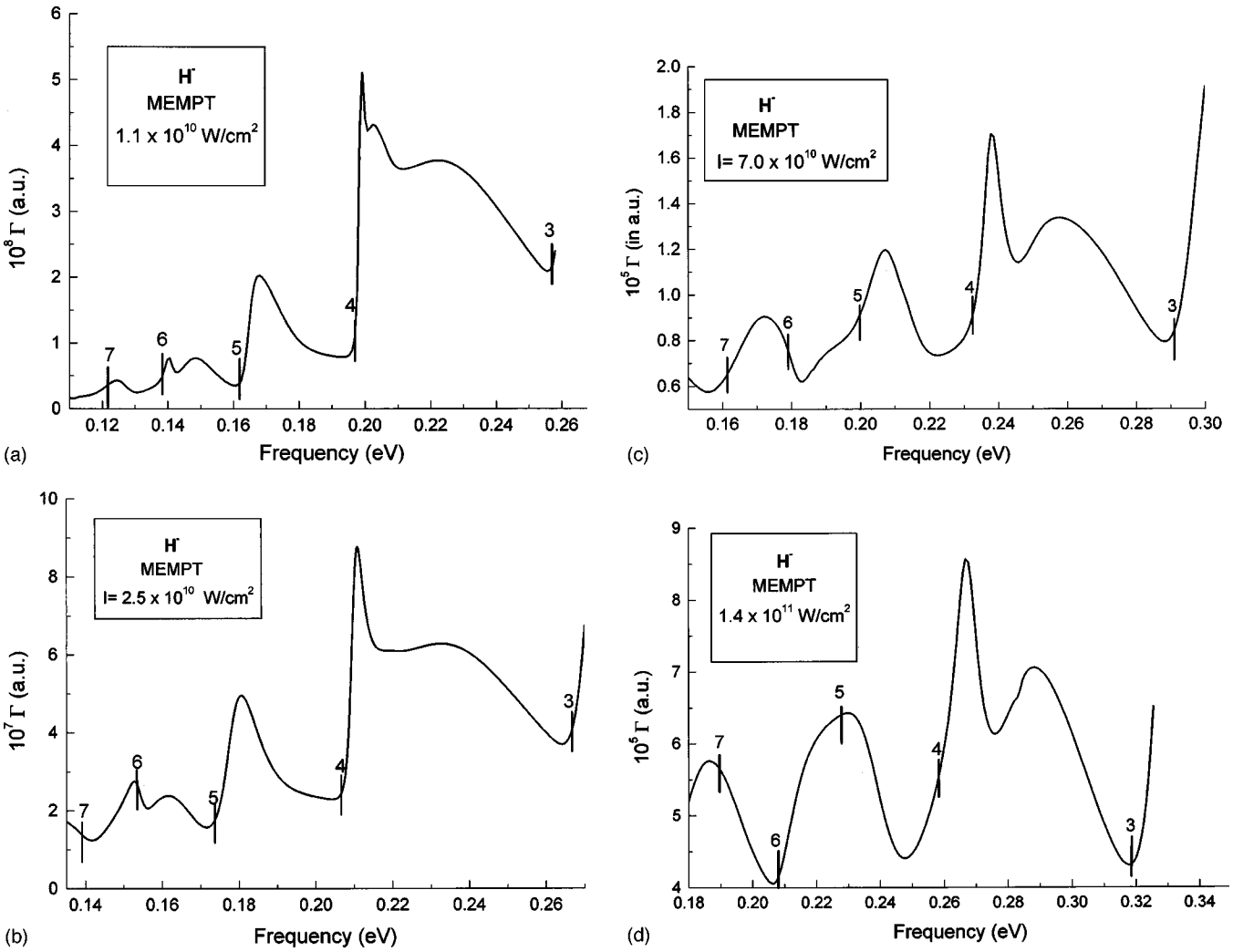

FIG. 2. (a) MEMPT results for MPEDRs in the frequency range between the seven-photon and three-photon thresholds and $I=1.1\times10^{10}$ W/cm^2. The structures in the six-photon and four-photon channels are due to the ^1S-^1D channel interference. (b) Same as in (a) for $I=2.5\times10^{10}$ W/cm^2. The structures are smoothed out. (c) Same as in (a) for $I=7.0\times10^{10}$ W/cm^2. The fingerprints of ^1S-^1D channel interference are present only in the four-photon channel. (d) Same as in (a)–(c) for $I=1.4\times10^{11}$ W/cm^2. Note that the positions of the photon thresholds have changed significantly from those of graph (a) relative to the form of the overall curve as well as in absolute terms.

nitudes of the rates are in general agreement. However, the shapes near threshold differ. Our results indicate the existence of a dip, which we attribute to the interference between the ^1S and ^1D channels. The effects of such channel interference were presented quantitatively in [8,9,6]. All calculations show the thresholds to be shifted to higher frequencies as intensity increases and to become less sharp. This phenomenon is general, and is further discussed in the next section where rates for detachment by more than three photons are presented.

Finally, in Table IV we compare our results with those of Telnov and Chu [27,28], which were obtained by implementing Floquet theory with complex scaling and a model potential. We point out that for the lowest three intensities (weak-field regime) the frequency of 0.755 eV (1640 nm) coincides with the position where the one-photon channel opens. As a result, the calculation is very sensitive to the value of the electron affinity used. Therefore, for this special case we avoid the comparison with the value given in [28]. For all the other values of ω and I, the MEMPT results and those obtained by the one-electron model Floquet calculations of Telnov and Chu [27,28] are in good agreement (the discrepancy ranging from 2% to 10%), and they show the same behavior as regards the maxima and the minima of the MPEDRs for the frequencies used: 0.650 eV (1.908 μm), 0.755 eV (1.640 μm), and 1.164 eV (1.064 μm).

C. Detachment by four, five, six, seven, or eight photons

To our knowledge, the existing results from nonperturbative calculations for this region are scarce. In contradistinction, the present quantitative study of MPEDRs for energies above the three-photon detachment threshold is extensive. The frequency-dependent MEMPT results are presented in Figs. 2(a)–2(d) for four intensities between 1.12×10^{10} and 1.4×10^{11} W/cm^2.

For intensities 1.1×10^{10} W/cm^2 [Fig. 2(a)] and 2.52×10^{10} W/cm^2 [Fig. 2(b)] the curves of the detachment rates

are similar as regards the appearance of minima and maxima, the existence of which was already discussed in Sec. IV B. The frequency where the n-photon detachment channel opens is calculated from $E(\text{binding})+U_p=n\omega$, $U_p=F^2/4\omega^2$, where F is the field strength. For these intensities, the ac shift is negligible compared to U_p.

On the other hand, when intensity increases to $7\times10^{10}\,\text{W/cm}^2$ [Fig. 2(c)] and $1.4\times10^{11}\,\text{W/cm}^2$ [Fig. 2(d)], the curve of the MPEDR vs frequency changes form. For intensity $7\times10^{10}\,\text{W/cm}^2$, when ω reaches the five-photon threshold, there is no sharp reduction of the detachment rate. Instead, only a change of the slope of the curve is observed. The same trend exists for the higher intensity of $1.4\times10^{11}\,\text{W/cm}^2$, as it is seen in Fig. 2(d). Now, the MPEDR curve shows no minimum either at the five-photon or at the seven-photon threshold. Our explanation of this phenomenon is that, at these high intensities, it is the higher-order contribution of photon channels with $n>6$ that dominates and not the six-photon channel. Therefore, the maxima and minima that appear at lower intensities as a direct result of the successive opening of the immediate photon channels are progressively reduced, or even washed out.

In support of this interpretation we turn to the results of Telnov and Chu [24] which were obtained for only one frequency (0.117 eV) and for three values of intensity. They report the partial widths for the n-photon channels. For the lowest value of intensity, $1.0\times10^{10}\,\text{W/cm}^2$, the eight-photon partial width is dominant, contributing 73% to the total rate. At this intensity, the energy difference is such that at least eight photons are required for electron detachment to occur. When intensity becomes $5.0\times10^{10}\,\text{W/cm}^2$, the minimum number of photons required for detachment is 11. The eleven photon width has a much lower contribution to the total rate—25%—while the higher channels of 12, 13, and 14 photons contribute 59%. Finally, at intensity $1.0\times10^{11}\,\text{W/cm}^2$ the minimum number of photons for detachment to take place is 16. This channel contributes 27% to the total width, while the sum of the widths of the higher ones, 17, 18, 19, and 20 contributes 50% [24]. These facts support the view that the aforementioned changes as a function of intensity of the nonperturbative MPEDRs result from the strong influence of photon channels of higher order. In fact, as it is clear from Fig. 1(c), indication of this effect appears already in the region of three- and two-photon detachment, where the rise of the rate at the channel threshold becomes less sharp as I increases. Eventually, when intensity aquires large enough values, the behavior of the MPEDR versus frequency changes form. As an example, in Fig. 3 we plot on a logarithmic scale the rate vs ω for four intensities between 2×10^{10} and $7\times10^{10}\,\text{W/cm}^2$. Our results show that the five-photon threshold behavior changes significantly with intensity.

The only frequency-dependent nonperturbative calculations of MPEDRs that we found in the literature for the region beyond the three-photon threshold are those of Dörr *et al.* [19]. Specifically, these authors plot the MPEDR vs $1/\omega$ for $I=1\times10^{11}\,\text{W/cm}^2$, a combination corresponding to four-photon detachment (Fig. 3 of [19]). Our Fig. 4 compares the MEMPT rates with those of [19], taken from their

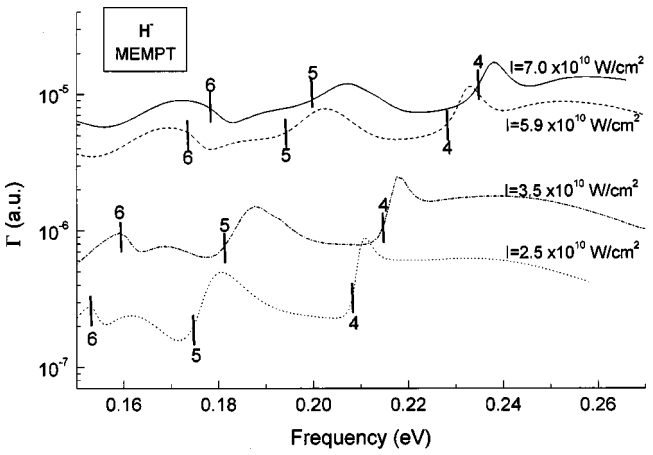

FIG. 3. Nonperturbative MPEDRs (a.u.) from the MEMPT, in logarithmic scale, for four intensities, covering the frequencies for detachment by 6, 5, and 4 photons.

plot. In both curves, there exist two peaks, which is the result of the contribution of the ^1S and ^1D channels and of their coupling [9(a)].

Finally, it is also possible to compare with and extend the early results published by Shakeshaft and Tang [29] only for one value of frequency, $\omega=0.234$ eV, and for five values of intensity. They used a one-electron parametrized Yukawa-type potential and Floquet theory. Table V compares their results with ours, the latter obtained for ten values of the intensity in the range between $2\times10^{10}\,\text{W/cm}^2$ and $1\times10^{11}\,\text{W/cm}^2$. The agreement is rather good. The MEMPT predicts that as I increases, the rate reaches a maximum around $I=6.3\times10^{10}\,\text{W/cm}^2$ and a minimum around $I=7.0\times10^{10}\,\text{W/cm}^2$, where the four photon-channel closes. The topic of the behavior of the MPEDRs as a function of intensity is discussed further in Sec. IV E.

D. The influence of doubly excited states

The frequencies used in this work are much smaller than 9–10 eV, where the first set of DES begins in the unper-

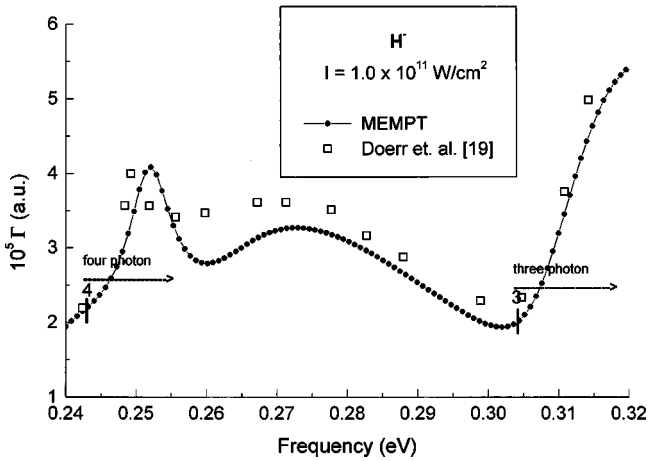

FIG. 4. Comparison of the MEMPT rates with the Floquet one-electron model calculations of [19] for four-photon detachment when $I=1.0\times10^{11}\,\text{W/cm}^2$.

TABLE V. MPEDRs of H^- (in a.u.) for $\omega=0.234$ eV. Reference [29]: Floquet theory with integral equations and a one-electron model potential. The MEMPT calculations reveal the smooth structure, as a function of I, caused by the existence of threshold at around $I=7.0\times10^{10}$ W/cm^2.

	Photodetachment rate (a.u.)	
I (W/cm^2)	MEMPT (This work)	Ref. [29]
2.00×10^{10}	$0.28(\pm0.01)\times10^{-6}$	
3.00×10^{10}	$0.11(\pm0.02)\times10^{-5}$	
4.48×10^{10}	$0.35(\pm0.02)\times10^{-5}$	0.44×10^{-5}
5.67×10^{10}	$0.80(\pm0.02)\times10^{-5}$	0.88×10^{-5}
6.28×10^{10}	$1.23(\pm0.02)\times10^{-5}$	
6.72×10^{10}	$1.15(\pm0.06)\times10^{-5}$	1.52×10^{-5}
6.86×10^{10}	$1.05(\pm0.01)\times10^{-5}$	1.30×10^{-5}
7.00×10^{10}	$1.04(\pm0.01)\times10^{-5}$	1.00×10^{-5}
8.00×10^{10}	$1.17(\pm0.01)\times10^{-5}$	
1.00×10^{11}	$1.94(\pm0.01)\times10^{-5}$	

turbed H^- spectrum. For example, if the frequency is 0.01 a.u., then more than 35 photons are required in order to reach the first ^1SDES. Therefore, one should expect that they do not play a significant role in the calculation of the MPEDRs. Indeed, our calculations showed that essentially identical results were obtained from two types of function spaces, one excluding the DES mentioned in Sec. III and one including them.

E. Channel closing and rates as a function of intensity

Obtaining quantitatively the MPEDR as a function of intensity (rather than frequency) is also interesting and experimentally feasible. We have already presented such results in Table V and we discussed other cases for two- and three-photon electron detachment in Sec. II.

As intensity increases, the ponderomotive shift causes the closing of photon channels. This effect was studied in [30,31] using solutions of the time-dependent Schrödinger equation (TDSE) which was solved under the assumption of a one-dimensional model for H^-. We did calculations for the same range of intensities ($1\times10^{10}-5\times10^{11}$ W/cm^2) and for the same value of laser frequency (0.29 eV). Our results are shown in Fig. 5 together with those of [30]. The results of [31] are very similar to the ones of [30]. The conclusion from this comparison is that these model calculations indeed revealed correctly the variations which are associated with the closing of channels. On the other hand, they did not produce an accurate picture either of the magnitude or of the shape of the curve of MREDR vs intensity. We note that in the MEMPT results, the closing of the channels is associated with dips at about $I=6.8\times10^{10}$ W/cm^2 (three photon), at about $I=2.4\times10^{11}$ W/cm^2 (four photon), and at $I=4.1\times10^{11}$ W/cm^2 (five photon).

Regarding the issue of channel closing, additional MEMPT calculations were carried out in order to compare with the R matrix Floquet results of Dörr *et al.* [26] who also

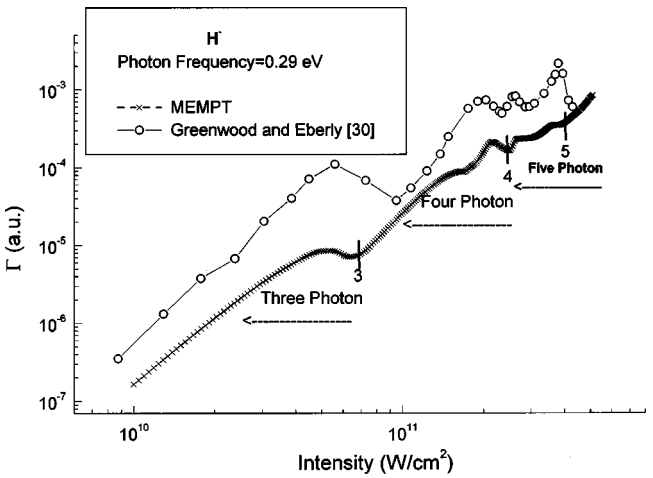

FIG. 5. Intensity dependence of MPEDRs (on logarithmic scale) for $\omega=0.29$ eV, with the results of [30] obtained from the solution of the time-dependent Schrödinger equation with a parametrized one-dimensional potential.

discussed this topic. Specifically, the intensity-dependent computations were done for $\omega=0.400$ eV, a value that is very near the frequency 0.405 eV (0.0149 a.u.) used in Ref. [26], Fig. 3. The results are shown in Fig. 6. The overall behavior of the MPEDRs is the same for both calculations. The MEMPT rates rise until I reaches 4.8×10^{10} W/cm^2 whereas the R-matrix Floquet rates of [26] rise until about $I=5.1\times10^{10}$ W/cm^2. Beyond these points the rate decreases until $I=6\times10^{10}$ W/cm^2, where the two-photon channel closes. Now, the three-photon channel starts dominating and the rate increases again. The magnitude of the rate is the same in both calculations.

Finally, we report that other MEMPT results, not given here for reasons of economy, are in agreement with the R-matrix Floquet calculation of Purvis *et al.* [32] which produced the rate for field parameters where the one-photon channel closes and with the one-electron model Floquet calculation of Dörr *et al.* [19] which obtained MPEDRs in the region where the two-photon channel closes.

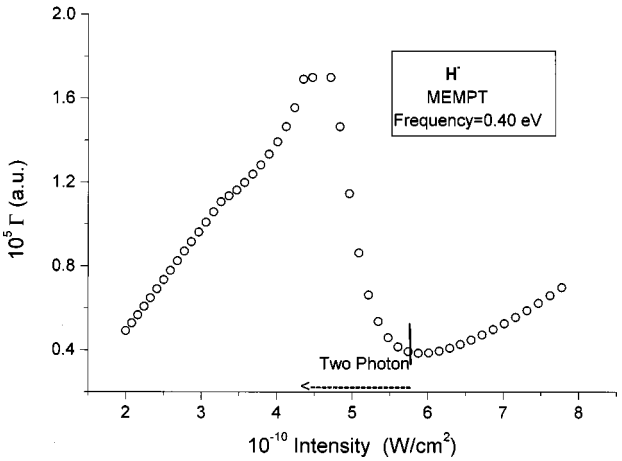

FIG. 6. Intensity dependence of MPEDRs for $\omega=0.40$ eV, where two-photon detachment takes place.

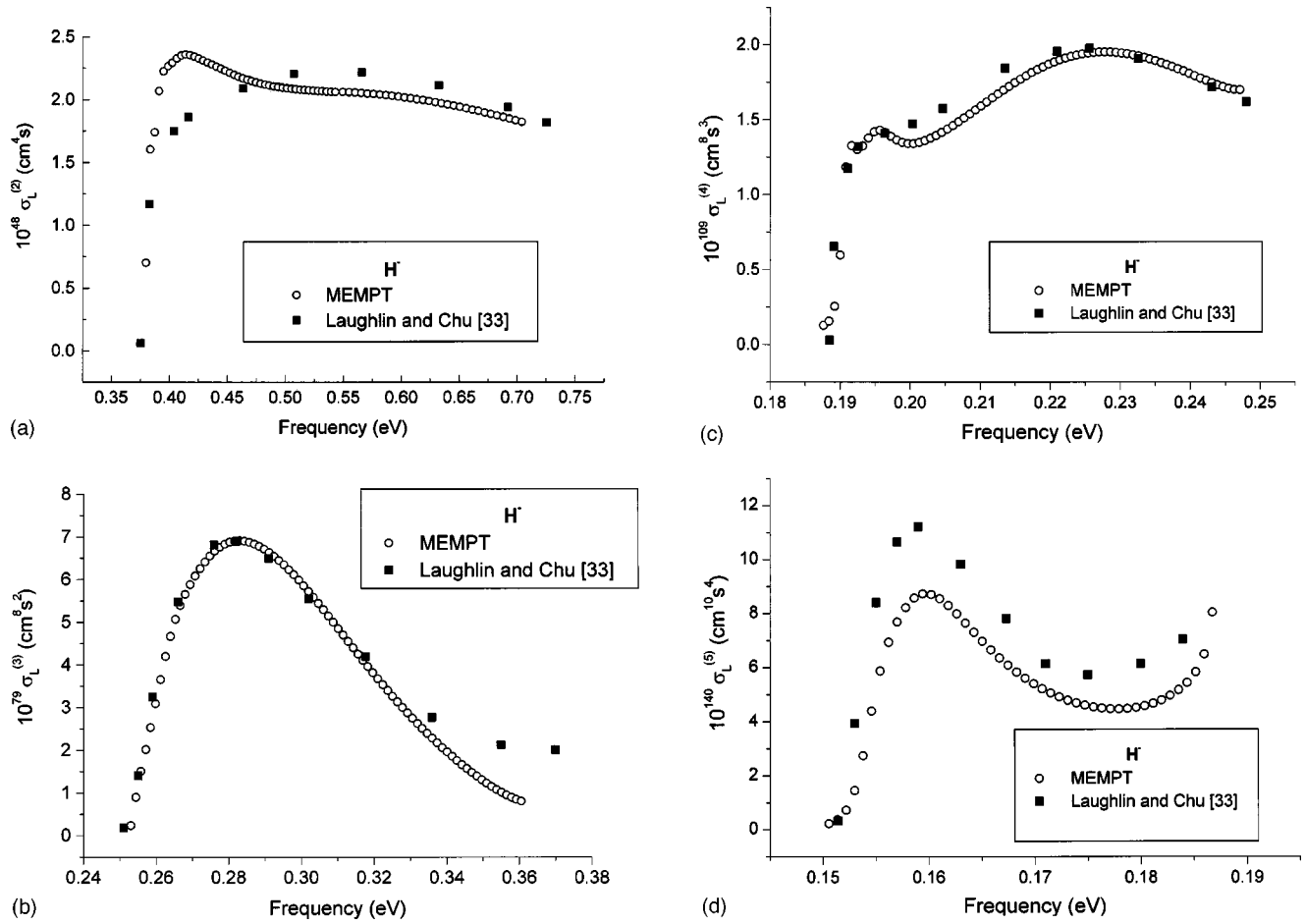

FIG. 7. (a) Two-photon generalized cross section from weak-field MEMPT calculations and comparison with the LOPT calculations of [33] which were carried out based on a parametrized one-electron model. There is a small discrepancy around $\omega = 0.40$ eV. (b) Same as in (a) for the three-photon generalized cross section. There is some discrepancy for ω larger than 0.34 eV. (c) Same as in (a) for the four-photon generalized cross section. Around $\omega = 0.195$ eV there is structure, which is much weaker and shifted in the results of [33]. The ponderomotive shift has been subtracted from our results since LOPT is independent of it. (d) Same as in (a) for the five-photon generalized cross section. The ponderomotive shift has been subtracted from our results since LOPT is independent of it.

F. Results for the weak-field regime

By choosing a series of small values of intensity, it is in principle possible to obtain from a MEMPT calculation MPEDRs which fall into the weak-field regime. However, because of numerical errors, the algorithms implementing the MEMPT cannot, at present, yield accurate values for the rates in H^- for intensities below 5×10^9 W/cm^2, and for photon energies which are smaller than the one required for five-photon detachment. For this reason, the MEMPT calculation of $\sigma^{(7)}$ and $\sigma^{(6)}$ has not been done here. On the other hand, our weak-field MEMPT calculations converged rather reliably for the cases of two-, three-, four-, and five-photon detachment rates. The corresponding $\sigma^{(n)}$, $n=2,3,4,5$, are presented in Figs. 7(a)–7(d) where they are compared with the LOPT results of Laughlin and Chu [33]. Laughlin and Chu obtained $\sigma^{(n)}$, $n=2-8$, by solving the corresponding inhomogeneous equations using a carefully parametrized one-electron model, a method that was applied to H^- by Adelman [34]for the calculation of $\sigma^{(2)}$. LOPT calculations for $\sigma^{(n)}$, $n=2-6$, were also done by van der Hart [35] using the summation method without the use of a one-electron model. Instead, he employed very large expansions of two-electron functions constructed from *B* splines, where the continuum functions are box normalized. van der Hart discussed comparisons with earlier results, for which the reader is referred to [35]. We note that his exposure of the contribution of the different final-state channels, ^1S, $^1P^o$, ^1D, etc., support the earlier remarks as to the phenomenon of channel interference [8,9(a)]. (Additional analysis of this threshold property will be given elsewhere.) Finally, another calculation in the weak-field regime was published by Dörr *et al.* [26] in which, however, the energies had to be adjusted empirically. Our comments regarding weak-field results such as the above are as follows.

We compare with the LOPT results of Laughlin and Chu [33], which we expect to be rather accurate on the whole, due to the method of solution and to the choice of the parametrized model. (This does not mean that results from other types of calculations are not reliable in general, especially far from threshold. For example, see the perturbative results of Proulx and Shakeshaft [36] for $\sigma^{(2)}$ and $\sigma^{(3)}$.) Such a comparison shows that there is an overall very good

TABLE VI. MPEDRs (in s^{-1}) from two MEMPT calculations (Ref. [9(a)] and this work) for $\omega = 0.354$ eV and four values of intensity for which electron detachment is achieved by three photons. The ratio rate/I^3 is supposed to be constant in the weak-field regime, where lowest-order perturbation theory (LOPT) applies. See [6].

	This work		Ref. [9(a)]	
I (W/cm^2)	Rate (s^{-1})	(Rate)/I^3 [s^{-1} (W cm^{-2})$^{-3}$]	Rate (s^{-1})	(Rate)/I^3 [s^{-1} (W cm^{-2})$^{-3}$]
1.75×10^{10}	7.92×10^{9}	1.48×10^{-21}	8.90×10^{9}	1.66×10^{-21}
7.00×10^{10}	5.46×10^{11}	1.59×10^{-21}	6.14×10^{11}	1.79×10^{-21}
1.58×10^{11}	5.41×10^{12}	1.38×10^{-21}	6.04×10^{12}	1.55×10^{-21}
2.80×10^{11}	8.03×10^{12}	3.66×10^{-22}	8.43×10^{12}	3.84×10^{-22}

agreement for $\sigma^{(3)}$ and $\sigma^{(4)}$, except around $\omega = 0.40$ eV for $\sigma^{(2)}$ and beyond $\omega = 0.34$ eV for $\sigma^{(3)}$, where small deviations are observed. For $\sigma^{(5)}$, the MEMPT values are a bit smaller but the two curves have the same shape. This difference is probably due to the fact that the value of the intensity, ($I = 6\times10^9$ W/cm^2), which was necessarily chosen for our calculations in order to obtain a reliable stability for the complex eigenvalue, was not small enough. If a well-converged MEMPT calculation with a smaller value of I were numerically possible, its results would be even closer to the LOPT ones of [33].

The case of $\sigma^{(2)}$ has been subjected to a number of calculations. Early discussions and comparisons were given in [9,17]. Figure 1 of [9(b)] shows the degree of discrepancy among various calculations at the time. The present MEMPT results agree with those of [33], except close to threshold, where the MEMPT results are slightly larger. It is worth pointing out that, in general, the *ab initio* computation of detachment rates at threshold are sensitive to the energy difference (binding energy) as well as to the quality of the wave functions. For example, consider the large-scale R-matrix Floquet calculations of Dörr *et al.* [26]. These authors found that without artificially shifting the energies, this type of calculation of the two- and three-photon rate for low intensities (1×10^9 W/cm^2) produced results which deviated from the final results. In fact, they had to move the lowest ^1S R-matrix pole from $-0.526\,427$ a.u. to $-0.528\,876$ a.u. in order to obtain the correct energy difference and, consequently, an acceptable rate. [Note that the chosen energy (-0.5289 a.u.) is below the exact energy of the H^- ^1S state.] Empirical corrections for the binding energy have also been necessary in other theoretical approaches to the calculation of $\sigma^{(n)}$ (e.g., [18]). Dörr *et al.* concluded ([26] p. 4493) that ''the semiempirical correction is very important to obtain an accurate detachment rate.''

Our calculations of MPEDRs, for all frequencies and intensities, employed the wave function and the (nearly exact) energy obtained from the ten-term MCHF calculation and no empirical fitting was done. Although we cannot establish the exact level of their accuracy, we can report that tests showed that the threshold behavior was stable to small changes in the intensity. A possible slight improvement could come from a small change in the magnitude of the MCHF1s orbital in the asymptotic region, which extends up to 45 a.u. [21].

According to LOPT, the n-photon detachment rate divided by I^n must be independent of the intensity. This relationship can be used to establish to a good approximation the values of intensity for each frequency at which the LOPT breaks down. Such an estimate was given in Table 4 of [9(a)] for $\omega = 0.013$ a.u. In Table VI we compare the present MEMPT results with those of [9(a)], corrected according to

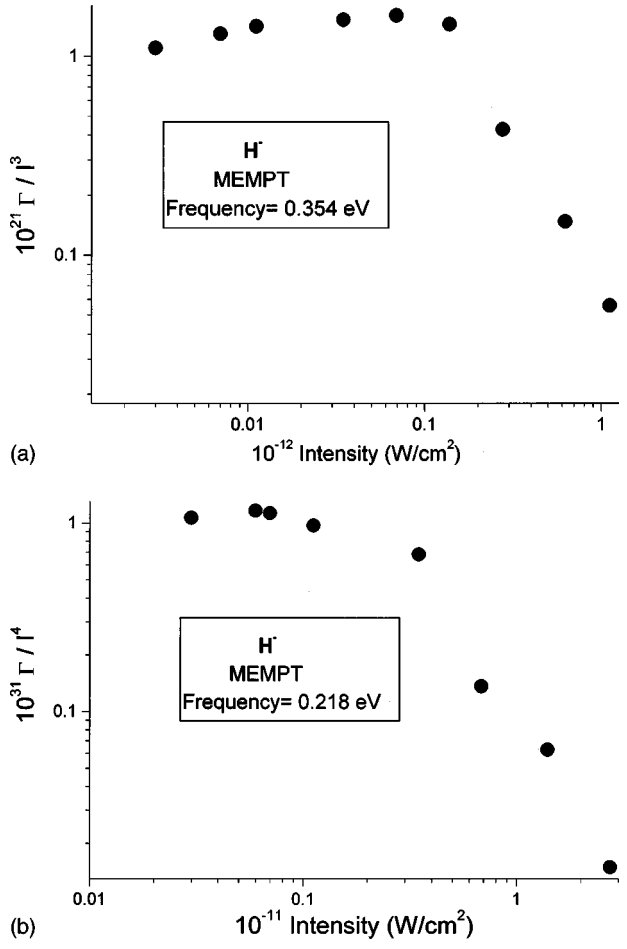

FIG. 8. (a) Rate/I^3 as a function of intensity for $\omega = 0.354$ eV, where at least three or four photons are needed for detachment to occur. The breakdown of the I^3 dependence appears after 1.1×10^{11} W/cm^2. (b) Same as in (a) for four- or five-photon detachment.

TABLE VII. Conclusions from the present MEMPT calculations as to the intensity range where the LOPT relation $\Gamma \sim I^k$ breaks down for five frequencies.

Frequency (eV)	Photons	Intensity (W/cm^2)
0.218	4	$4-5\times10^{9}$
0.223	4	$5-6\times10^{9}$
0.326	3	$7-10\times10^{10}$
0.354	3	$9-11\times10^{10}$
0.490	2	$2-3\times10^{11}$
0.571	2	$2-3\times10^{11}$

[6]. The agreement is good. Additional results are given in Figs. 8(a) and 8(b) where we plot this quantity G/I^n vs I. The breakdown occurs at about $I=(4-5)\times10^9$ W/cm^2 for four photons and at about $I=(9-11)\times10^{10}$ W/cm^2 for three photons. Table VII contains a number of results showing the values of ω and I where the perturbative power law is expected to breakdown.

V. CONCLUSION

The plethora of results presented here for the various MPEDR ''spectra'' of the system ''*H plus ac-field*'' complement and enrich the existing information for the weak- and especially for the strong-field regimes. Furthermore, in combination with the recently published study of the isoelectronic ''*He plus ac-field*'' system [3], the present implementation of the MEMPT indicates the way in which the problem of computing the nonlinear response of polyelectronic atomic states of arbitrary structures in ac fields can be treated within a nonperturbative framework economically as well as accurately. For example, consider the calculation of the MPEDR spectrum of an open-shell negative ion, say O^-, for a range of experimentally feasible frequencies and intensities. (The electron affinity of O^- is 1.46 eV.) The computational implementation of the MEMPT will consist of the following main steps. (i) Calculate the appropriate correlated nine-electron wave functions Ψ_i and the eight-electron wave functions (core terms) of X_j of Eq. (2), with real coordinates. If necessary, include configurations representing doubly excited states and core polarization. According to [20], these bound functions are compact, consisting of a numerical MCHF solution for the zero-order reference wave function and a variationally optimized part for the remaining correlation. (Of course, the MCHF calculation can in principle be enlarged as much as possible, so as to render the addition of configurations with analytic virtual orbitals unnecessary.) (ii) Couple to the eight-electron final-state wave functions one-electron complex orbitals of a complex coordinate, according to Eqs. (8)–(10), and construct the MEMPT matrix, using the form (2) and the Hamiltonian (1). (iii) Solve iteratively for the state-specific complex eigenvalue for each pair of (I,ω), following the method presented in [9(a),10,3]. Of course, although the main steps are indicated by the theory, it is a matter of considerable additional experience to understand the suitability of L^2 complex functions as to the representation of the contribution of the multichannel continuous spectrum to the field-dressed resonance eigenfunction in many-electron atoms for each pair (I,ω).

[1] J. N. Silverman and C. A. Nicolaides, Chem. Phys. Lett. **153**, 61 (1988); **184**, 321 (1991).

[2] M. Bylicki, S. I. Themelis, and C. A. Nicolaides, J. Phys. B **27**, 2741 (1994).

[3] Th. Mercouris, S. I. Themelis, and C. A. Nicolaides, Phys. Rev. A **61**, 013407 (2000).

[4] S. I. Themelis, Th. Mercouris, and C. A. Nicolaides, Phys. Rev. A **61**, 024101 (2000).

[5] (a) C. Y. Tang, H. C. Bryant, P. G. Harris, A. H. Mohagheghi, R. A. Reeder, H. Sharifian, H. Toutounchi, C. R. Quick, J. B. Donahue, S. Cohen, and W. W. Smith, Phys. Rev. Lett. **66**, 3124 (1991); P. Balling, H. H. Andersen, C. A. Brodie, U. V. Pedersen, V. V. Petrunin, M. K. Raarup, P. Steiner, and T. Andersen, Phys. Rev. A **61**, 022702 (2000); (b) H. C. Bryant, V. Yuan, C. R. Hummer, W. W. Smith, S. Cohen, W. P. Reinhardt, and L. Overman, Phys. Rev. Lett. **58**, 2412 (1987).

[6] This work has given us the opportunity of checking the earlier MEMPT calculations on H^-. (See Refs. [7–9(a)].) Two errors affecting the then-published nonperturbative MPEDRs were found. The first is superficial. It has to do with the fact that the values of the intensity which are given in the figures of Refs. [7–9(a)] are larger by a factor of 2 than the ones corresponding to the actual calculation. For example, the MPEDRs of Table 3 of [9(a)] correspond to $I=0.7\times10^{11}$ W/cm^2 and not to 1.4×10^{11} W/cm^2, as written in the caption. On the other hand, the values of the field strength which are also given in some of the figures, are correct. The explanation is that in the conversion from F (field strength) to I (peak intensity), in a.u., a factor of 2 was inadvertently left in the code, thereby giving $2\times I$ as the value of the intensity. The second error, which is also mentioned in the main text, has to do with the lack of capacity of the MEMPT algorithms to obtain stable and reliable complex eigenvalues with imaginary parts (decay widths) smaller than about 10^{-11} a.u. This fact led to false indication of proper convergence in the computations of [7] (CO_2 frequencies), except for $I=1.25\times10^{10}$ W/cm^2.

[7] Th. Mercouris and C. A. Nicolaides, J. Phys. B **21**, L285 (1988).

[8] C. A. Nicolaides and Th. Mercouris, Chem. Phys. Lett. **159**, 45 (1989).

[9] (a) Th. Mercouris and C. A. Nicolaides, J. Phys. B **23**, 2037 (1990); (b) Phys. Rev. A **45**, 2116 (1992).

[10] C. A. Nicolaides, Th. Mercouris, and G. Aspromallis, J. Opt. Soc. Am. B **7**, 494 (1990).

[11] Th. Mercouris and C. A. Nicolaides, J. Phys. B **24**, L54 (1990).

[12] Th. Mercouris and C. A. Nicolaides, J. Phys. B **24**, L557 (1991).

[13] M. G. J. Fink and P. Zoller, J. Phys. B **18**, L373 (1985).
[14] M. Crance and M. Aymar, J. Phys. B **18**, 3529 (1985).
[15] P. A. Golovinskii and B. A. Zon, Bull. Acad. Sci. USSR, Phys. Ser. (Engl. Transl.) **45**, 12 (1981).
[16] N. B. Delone, Yu I. Kiyan, V. P. Krainov and V. I. Inglushev, Opt. Spectrosk. **58**, 262 (1985) [Opt. Spectrosc. **58**, 157 (1985)].
[17] S. Geltman, Phys. Rev. A **43**, 4930 (1991).
[18] C. R. Liu, B. Gao, and A. F. Starace, Phys. Rev. A **46**, 5985 (1992).
[19] M. Dörr, R. M. Potvliege, D. Proulx and R. Shakeshaft, Phys. Rev. A **42**, 4138 (1990).
[20] C. A. Nicolaides, Int. J. Quantum Chem. **60**, 119 (1996); **71**, 209 (1999).
[21] C. A. Nicolaides, C. Haritos, and Th. Mercouris, J. Phys. B **33**, 2733 (2000).
[22] C. Froese-Fischer, Comput. Phys. Commun. **14**, 145 (1978).
[23] M. Bylicki and C. A. Nicolaides, Phys. Rev. A **61**, 052508 (2000); **61**, 052509 (2000).
[24] D. A. Telnov and S. I. Chu, Phys. Rev. A **50**, 4099 (1994).
[25] J. Wang, S. I. Chu, and C. Laughlin, Phys. Rev. A **50**, 3208 (1994).
[26] M. Dörr, J. Purvis, M. Terao-Dunseath, P. G. Burke, C. J. Joachain, and C. J. Noble, J. Phys. B **28**, 4481 (1995).
[27] D. A. Telnov and S. I. Chu, J. Phys. B **29**, 4401 (1996).
[28] D. A. Telnov and S. I. Chu, Phys. Rev. A **59**, 2864 (1999).
[29] R. Shakeshaft and X. Tang, Phys. Rev. A **36**, 3193 (1987).
[30] W. G. Greenwood and J. H. Eberly, Phys. Rev. A **43**, 525 (1991); R. Grobe and J. H. Eberly, *ibid.* **48**, 4664 (1993).
[31] G. Scharf, K. Sonnenmoser, and W. F. Wreszinski, Phys. Rev. A **44**, 3250 (1991).
[32] J. Purvis, M. Dörr, M. Terao-Dunseath, C. J. Joachain, P. G. Burke, and C. J. Noble, Phys. Rev. Lett. **24**, 3943 (1993).
[33] C. Laughlin and S. I. Chu, Phys. Rev. A **48**, 4654 (1993).
[34] S. A. Adelman, J. Phys. B **6**, 1986 (1973).
[35] H. W. van der Hart, Phys. Rev. A **50**, 2508 (1994).
[36] D. Proulx and R. Shakeshaft, Phys. Rev. A **46**, R2221 (1992).